International Journal of Biological, Life and Agricultural Sciences
ISSN: 2415-6612
Vol:12, No:10, 2018

A Finite Element/Finite Volume Method for Dam-Break Flows over Deformable Beds

Alia Alghosoun, Ashraf Osman, Mohammed Seaid

***Abstract*—**A coupled two-layer finite volume/finite element method was proposed for solving dam-break flow problem over deformable beds. The governing equations consist of the well-balanced two-layer shallow water equations for the water flow and a linear elastic model for the bed deformations. Deformations in the topography can be caused by a brutal localized force or simply by a class of sliding displacements on the bathymetry. This deformation in the bed is a source of perturbations, on the water surface generating water waves which propagate with different amplitudes and frequencies. Coupling conditions at the interface are also investigated in the current study and two mesh procedure is proposed for the transfer of information through the interface. In the present work a new procedure is implemented at the soil-water interface using the finite element and two-layer finite volume meshes with a conservative distribution of the forces at their intersections. The finite element method employs quadratic elements in an unstructured triangular mesh and the finite volume method uses the Rusanove to reconstruct the numerical fluxes. The numerical coupled method is highly efficient, accurate, well balanced, and it can handle complex geometries as well as rapidly varying flows. Numerical results are presented for several test examples of dam-break flows over deformable beds. Mesh convergence study is performed for both methods, the overall model provides new insight into the problems at minimal computational cost.

***Keywords*—**Dam-break flows, deformable beds, finite element method, finite volume method, linear elasticity, Shallow water equations.

I. Introduction

MODELING of the wave-seabed interaction has been one of the oldest challenges facing geotechnical engineers, as it is important to design offshore engineering projects like pipelines and break waters. In addition to the floating/sinking of objects on the seabed like mines or wrecked ships, the design of offshore structures under different environmental conditions has become more essinitial, challenging and critical. Experiments [9] and numerical simulations [12] have been done to try understanding this complicated process. Analytical models were described the sea response [2]–[4], [7]. However, the majority of these models assume the pressure on the bed-water interface using the wave theory [8], [10], this is applicable as initial approximation for many cases if there is only seabed and water wave interaction,however, the water flow around any object will be three-dimensional (3D) and it is not easy to be solved using the wave theory.

A. Alghosoun is with department of Engineering, University of Durham, South Road, Durham DH1 3LE, UK (e-mail: alia.r.al-ghosoun@durham.ac.uk).

A. Osman is with is with department of Engineering, University of Durham, South Road, Durham DH1 3LE, UK (e-mail: ashraf.osman@durham.ac.uk).

M. Seaid is with department of Engineering , University of Durham, South Road, Durham DH1 3LE, UK (e-mail: m.seaid@durham.ac.uk).

This problem has attracted more and more attentions in engineering and coastal, many experimental studies have also been carried out. Authors in [1] carried out a series of two-dimensional wave tank experiments, to investigate the relationships through the waves, the dynamic stresses within the seabed and the pressure on interface. A one dimensional cylindrical experiment were done to study the wave driven oscillatory pore pressure in a sandy seabed were carried out [5]. Although many efforts have been made in the previous studies, the problem of the bed-wave interaction is still not completely understood, due to the complicated mechanics of seabed response under the ocean waves.

In this study we aim to tackle the problems of wave-seabed interaction, as gaining more accurate results for more complex beds geometry. To achieve this we utilize a coupled model to simulate the two layers shallow water induced by elastic deformations in the bed topography. The perturbation on the free-surface is assumed to be caused by a sudden changes in the bottom beds. Attention is concentrated on the development of a simple and accurate representation of the interaction between water waves and bed deformation to simulate practical shallow water waves and bed deformations without relying on complex differential with free boundary conditions.

This paper is structured as follows: A brief overview of the governing equations considered in this study is given in Section II. A short review of the numerical methods used is outlined in Section III. In Section IV results of benchmarks and novel testing are presented. Finally in Section V some conclusions are drawn.

II. Modeling of Dam Break over Deformable Beds

In this section a coupled two-dimensional equations of linear elasticity for the soil bed and the one-dimensional two-layer shallow water equations for the water flow are utilized, the governing equations for each system are described in the next subsections:

A. Equations for Water Flow

In the current study we are interested in solving the hydraulic flows occuring on the water free-surface, The one-dimensional two-layer shallow water equations with different densities, ρ_1, ρ_2, as $\rho_1 < \rho_2$ given as:

$$\frac{\partial h_1}{\partial t} + \frac{\partial}{\partial x}(h_1 u_1) = 0,$$

$$\frac{\partial}{\partial t}(h_1u_1)+\frac{\partial}{\partial x}(h_1u_1^2+\frac{1}{2}gh_1^2)=-gh_1\frac{\partial h_2}{\partial x}-gh_1\frac{\partial z}{\partial x},$$
$$\frac{\partial h_2}{\partial t}+\frac{\partial}{\partial x}(h_2u_2)=0, \quad (1)$$
$$\frac{\partial}{\partial t}(h_2u_2)+\frac{\partial}{\partial x}(h_2u_2^2+\frac{1}{2}gh_2^2)=-\frac{\rho_1}{\rho_2}gh_2\frac{\partial h_1}{\partial x}-gh_2\frac{\partial z}{\partial x}$$

where u_1, u_2 are the water speed in the first and second layer respectively, h_1,h_2 are the water height in the first and seconf layer respectively, and g is the gravity constant. Fig. 1 shows the system characterestics for more illustrations.

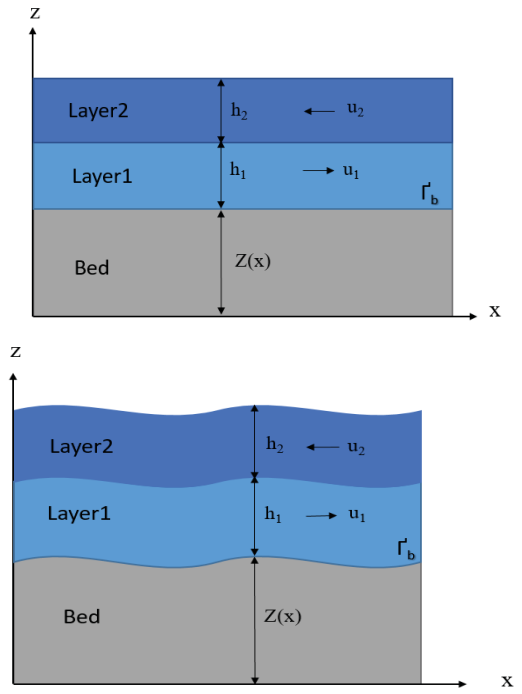

Fig. 1 Illustration of a coupled system

The main advantage of the above system is the fact, that the two layers shallow water models avoids the expensive computational three dimensional Navier-Stokes equations, and obtains satisfied horizental flow velocities as vertical velocities are relatively small, on the other hand it avoids the drawback of single layer shallow water in missing some physical dynamics in the vertical motion.

B. Equations for Bed Deformations

In solid mechanics the conservation laws produce three important governing equations, mass, linear momentum and energy conservations, the linear elasticity and steady slow incompressible viscous flows governing equations are summarized as:

The equation of equilibrium, which given by:

$$\nabla\cdot\sigma+f=0 \quad (2)$$

in which σ is the stress tensor and f the body force. The displacement vector is denoted by u and the infinitesimal strain is then defined by:

$$\epsilon=\frac{1}{2}\big(\nabla u+(\nabla u)^T\big) \quad (3)$$

and the **constitutive equation** reads:

$$\sigma=\frac{\nu E}{(1+\nu)(1-2\nu)}(\nabla\cdot u)I+\frac{E}{1+\nu}\epsilon \quad (4)$$

In which E is the Youngs modulus and ν is poisson's ratio. Interaction between flow and soil domain through the interface as shown in Fig. 2.

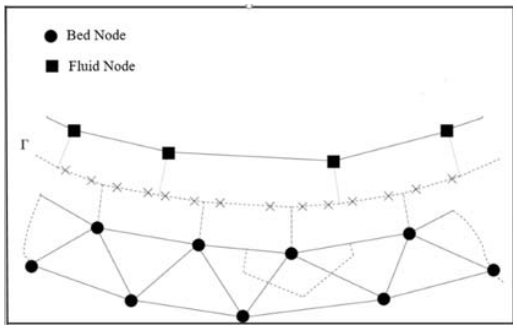

Fig. 2 Interaction between flow and soil domain through the interface

III. Numerical Procedures

The two layers shallow water equations are investigated in this part, as a non-conservative system compared to the single layer shallow water model.

For ease the governing equations in the previous model were re-arranged into vector form:

$$\frac{\partial\mathbf{W}}{\partial t}+\frac{\partial\mathbf{F}(\mathbf{W})}{\partial x}=\mathbf{Q}(\mathbf{W}) \quad (5)$$

where $\mathbf{W}$ is the vector of conserved variables, $\mathbf{F}(\mathbf{W})$ is the vector of flux functions $\mathbf{Q}$ is the vectors of source terms.

$$\mathbf{W}=\begin{bmatrix}h_1\\h_1u_1\\h_2\\h_2u_2\end{bmatrix},\qquad \mathbf{F}(\mathbf{W})=\begin{bmatrix}h_1u_1\\h_1u_1^2+\frac{1}{2}gh_1^2\\h_2u_2\\h_2u_2^2+\frac{1}{2}gh_2^2\end{bmatrix}, \quad (6)$$

$$\mathbf{Q}(\mathbf{W})=\begin{bmatrix}0\\-gh_1\frac{\partial h_2}{\partial x}-gh_1\frac{\partial z}{\partial x}\\0\\-rgh_2\frac{\partial h_1}{\partial x}-gh_2\frac{\partial z}{\partial x}\end{bmatrix} \quad (7)$$

With the ratio $r=\frac{\rho_1}{\rho_2}$. For hydraulic applications with $r\approx 1$, and $u_1\approx u_2$, a first order approximation of the eigen values can be obtained [6]:

$$\lambda_1\approx U_m-\sqrt{g(h_1+h_2)},$$
$$\lambda_2\approx U_m+\sqrt{g(h_1+h_2)},$$
$$\lambda_3\approx U_c-\sqrt{(1-r)g\frac{h_1h_2}{h_1+h_2}\big(1-\frac{(u_2-u_1)^2}{(1-r)g(h_1+h_2)}\big)} \quad (8)$$

$$\lambda_4 \approx U_c + \sqrt{(1-r)g\frac{h_1 h_2}{h_1+h_2}\big(1-\frac{(u_2-u_1)^2}{(1-r)g(h_1+h_2)}\big)}$$

where:

$U_m = \frac{h_1u_1+h_2u_2}{h_1+h_2}$, and $U_c = \frac{h_1u_1+h_2u_2}{h_1+h_2}$.

The shallow water domain is discretized into group of control volumes $[x_{i-\frac{1}{2}}, x_{i+\frac{1}{2}}]$, with uniform sizes $\triangle x$ and then divide the temporal domain into subintervals $[t_n, t_{n+1}]$ with step size $\triangle t$. The previous system was integrated in space over a control volume and obtain the relation:

$$\frac{d\mathbf{W}_i}{dt} + \frac{\mathbf{F}_{i+\frac{1}{2}} - \mathbf{F}_{i-\frac{1}{2}}}{\triangle x} = \mathbf{Q}_i \tag{9}$$

where $\mathbf{W}_i(t)$ is the averaged solution $\mathbf{W}$ in the control volume at time t.

$$\mathbf{W}_i(t) = \frac{1}{\triangle x}\int_{x_{i-\frac{1}{2}}}^{x_{i+\frac{1}{2}}} \mathbf{W}(t,x)dx \tag{10}$$

$$\mathbf{W}_i^{n+1} = \mathbf{W}_i - \triangle t\ \frac{\mathbf{F}_{i+\frac{1}{2}} - \mathbf{F}_{i-\frac{1}{2}}}{\triangle x} + \triangle t\mathbf{Q}_i \tag{11}$$

A. Two Dimensional Linear Elastic Finite Element

The deformations occur in plane strains, where the fundamental relationship for linear elastic finite element is :

$$[\mathbf{K}][\mathbf{u}] = [\mathbf{F}] \tag{12}$$

where $\mathbf{F}$ is the load vector, $\mathbf{K}$ is element stiffness matrix , which is for an arbitrary element is obtained from:

$$\mathbf{K} = \int_\Omega \int \mathbf{B}^T\ E\ \mathbf{B}\ j\ d\xi\ d\eta \tag{13}$$

as $\mathbf{B}$ is the strain deformation matrix, j is the determinant of the jacobian matrix, given as $\mathbf{J} = \frac{\partial(x,y)}{\partial(\xi,\eta)}$, $\mathbf{u}$ is the displacement vector. This is typically solved by calculating the stiffness matrix, inverting it, then solving for displacement. Finally the stress-strain relationship is given by:

$$[\sigma] = [\mathbf{D}][\epsilon] \tag{14}$$

where ϵ is the strain vector, found from displacement components, $\mathbf{D}$ is the elastic symmetric component.

IV. Applications and Numerical Results

To examine the performance of our system we present numerical results for several test examples. We illustrate the accuracy for both two-layer shallow water system and the linear elastic finite element model. As with all explicit time stepping methods the time step is specified according to the Courant-Friedrichs-Lewy (CFL) condition as:

$$\triangle t = C_r \frac{\triangle x}{max\ \ |\ \lambda_k\ |} \tag{15}$$

where λ_k,k=1,2,3,4 are the approximated eigen values, and C_r is a constant to be choosen less than unity. In all the examples presented in this paper the courant number is set to 0.5 and the time step Δt is adjusted at each step according to the stability condition.

A. Lock Exchange Problem

The accuracy of the proposed finite element and two layers shallow water were checked for validation. To test the two layers shallow water we solve the Lock exchange problem, where in this example the two layers are initially seperated-the lighter water is on the left, while the heavier one is on the right:

$$\big(h_1(x,0), q_1(x,0), h_2(x,0), q_2(x,0)\big) = \begin{cases} -Z(x), 0, 0, 0 & x<0 \\ 0, 0, -Z(x), 0 & x>0 \end{cases}$$

where the bottom topography is Gaussian-Shape function Z(x) = $e^{-x^2} - 2$. The gravitational constant is $g = 9.81$, and the density ration $r = 0.98$. The computational domain is [-3,3], and the boundary conditions are $q_1 = -q_2$ at each end of the interval. The problem solved using different numbers of grid points and the L^1-error were calculated compared to very refined (12,800 grid points) mesh and the errors, rate of convergence and the computational time are shown in Table I.

TABLE I
Errors for the Lax-Friedrich Accuracy Test Problem Using Different Gridpoints

N	Error in H	Rate	CPU
100	6.55E-2	-	0.15
200	2.2E-2	1.07	0.35
400	7.7E-3	1.07	1.08
800	4.0E-3	1.13	3.22
1600	2.4E-3	1.2	6.22

As from the above table the mesh shows very good rate of convergence, and the method is fist order. Next we examine the finite element method by comparing the numerical vertical and horizental displacements results for a homogenous and isotropic rectangular domain with 100 m length and 10m hight to the analytical solution [11] assuming the Young's modulus of elasticity is 10,000 Mpa, and the poisons ratio = 0.2, which can be clearly shown in Fig. 3.

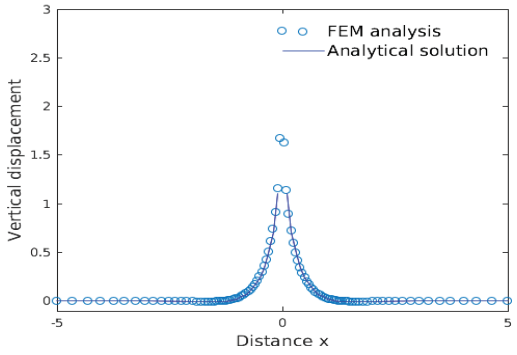

Fig. 3 Finite element displacement compared to the analytical solution

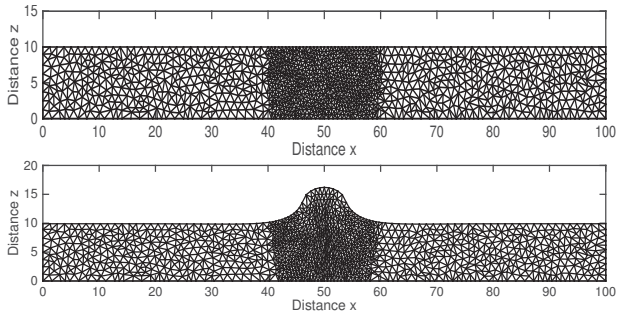

Fig. 4 Mesh before and after deformation

B. Free-Surface Flows with Raised Bed

In this example a free-surface flows over a rectangular domain with 100 m length and 10 m hight subjected to 1500 N tension force, using quadratic six nodes finite element , which generally provides higher accuracy in simulations as there are more nodes compared to number of elements. However, this required a greater memory and approximately doubled simulation time. It is therefore reasonable to proceed using the results from the coarse triangular mesh model because this mesh type tended to have fewer nodes. It can be seen that the mesh is finer near the load points and where largest deformations are likely to occur. Fig. 5 represents the mesh before and after deformation. For the water simulation, a sudden deformation was introduced at t=0.1 second, the water waves experiencing a smooth dam break as a response to this deformations, the water hight keep decreasing till reach the steady state. Fig. 6 presents the wave propagation at different time steps, hence the gray portion is the soil deformationa and the blue portion represents the two layers shallow water waves.

The two main dialary stresses are shown in Fig. 6, and it can be clearly shown that the maximum stresses values in the region of maximum deformation and symmetrical around it.

V. Conclusions

A simple and accurate approach to couple free-surface flows with bed deformations has been presented. The governing equations consist on coupling the nonlinear shallow water equations to the linear equations for elasticity. The coupling conditions between the two models is achieved through the interface between the two bodies and only the updated bathymetry is required for the free-surface simulations. As numerical solvers we have considered a conservative finite volume method for the free-surface flow and a robust finite element method for the bed deformation. The new method has several advantages. First, it can solve steady flows over irregular beds without large numerical errors, thus demonstrating that the proposed scheme achieves perfect numerical balance of the gradient fluxes and the source terms. Second, it can compute the numerical flux corresponding to the real state of water flow without relying on Riemann problem solvers. Third, reasonable accuracy can be obtained easily and no special treatment is needed to maintain a numerical

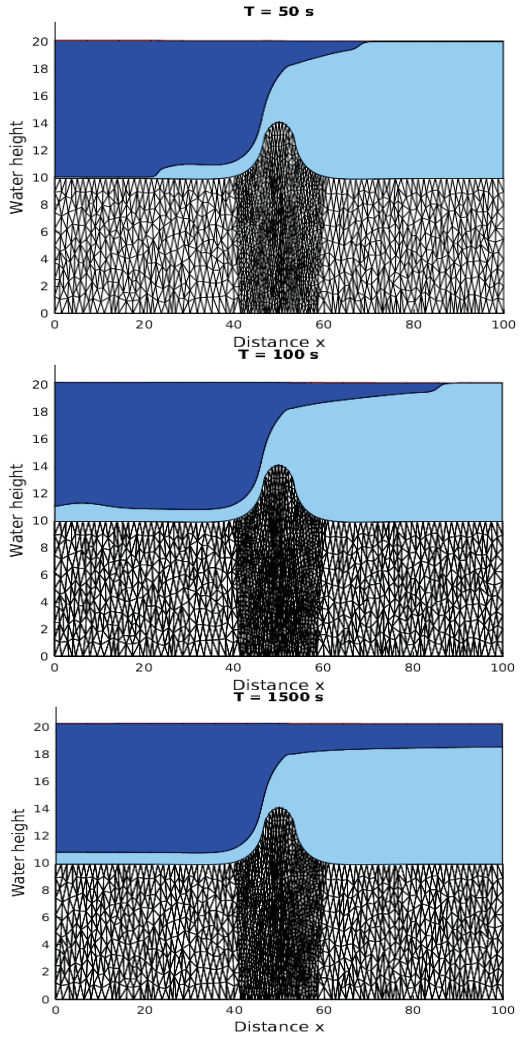

Fig. 5 Water height at different time steps

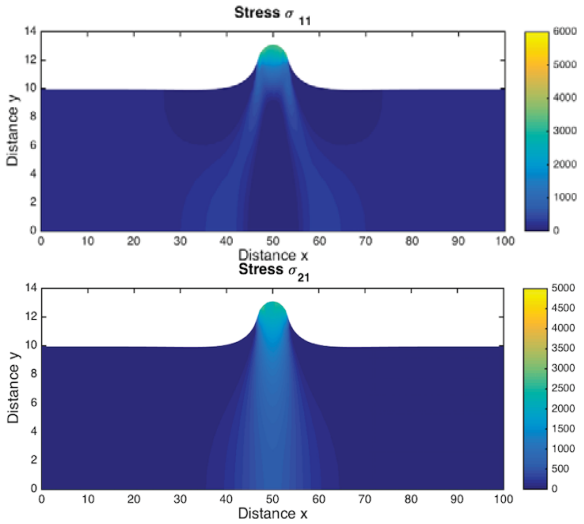

Fig. 6 Stresses σ_{11}, σ_{21}

balance, because it is performed automatically in the integrated numerical flux function. Finally, the proposed approach does not require either nonlinear solution of algebraic equations or special front tracking techniques. Furthermore, it has strong applicability to various problems in shallow water flows over deformed beds as shown in the numerical results. The proposed approach has been numerically examined for the test example of free-surface flow problems on different topographies.

REFERENCES

[1] M. Banner and W.Peirson. Wave breaking onset and strength for two dimensional deep water wave groups. *J. Fluid Mech*, 585:93–115, 2007.
[2] A. Bermudez, J. Ferrin, L. Savedra, and M. Vazques-Cendon. A projection hybrid finite volume/element method for low-mach number flows. *J. Comput. Phys*, 271:360–378, 2014.
[3] H. Dark and L. Stewart. An analytical model for predicting underwater noise radiated from offshore pile driving. In *Proceedings of the fifth Asia pacific congress on computational mechanics Conference*, pages 2–20, December 2013.
[4] H. Dark and L. Stewart. An analytical model for wind-driven arctic summer sea ice drift. *The cryosphere*, 10:227–244, 2016.
[5] U. Drahne, N. Goseberg, S. Vatar, N. Beisiegal, and J. Behrens. An experimental and numerical study of long wave run-up on a plane beach. *Journal of marine science and engineering*, 4:1–23, 2016.
[6] M. Le Gal, D. Violeau, R. Ata, and X. Wang. Shallow water numerical models for the 1947 gisborne and 2011 tohoku-oki tsunami with kinematic seismic generation. *Coastal Engineering*, 139:1–15, 2018.
[7] J. Greenberg and A. Leroux. A well-balanced scheme for the numerical processing of source terms in hyperbolic equations. *SIAM J.Numer.Anal*, 33:1–16, 2006.
[8] R. Harcourt. A second moment model of langmuir turbulance. *J. Phys. Oceanogr*, 43:673–697, 2013.
[9] C. Liao, Z. Lin, Y. Guo, and D. Jeng. Coupling model for waves propagating over a porous seabed. *Theoritical and applied mechanics letters*, 5:85–88, 2015.
[10] C. Ng. Water waves over a muddy bed: a two-layer strokes boundary layer model. *Coastal engineering*, 40:221–242, 2000.
[11] H. Poulos and E. Davis. *Elastic solutions for soil and rock mechanics*. The University of Sydney, Australia, 1991.
[12] D. Tong, C. Liao, J. Chen, and Q. Zhang. Numerical simulations of a sandy seabed response to water surface waves propagating on current. *Journal of marine science and engineering*, 6:1–14, 2018.